



HAL
open science

Characterization of tuna dark muscle protein isolate

Trong Bach Nguyen, Laurine Mule Mueni, Tran Nu Thanh Viet Bui, Huynh
Nguyen Duy Bao, Nguyen Thi Kim Cuc, Taco Nicolai

► To cite this version:

Trong Bach Nguyen, Laurine Mule Mueni, Tran Nu Thanh Viet Bui, Huynh Nguyen Duy Bao, Nguyen Thi Kim Cuc, et al.. Characterization of tuna dark muscle protein isolate. *Journal of Food Processing and Preservation*, 2022, 46 (8), <10.1111/jfpp.16753>. <hal-03805129>

HAL Id: hal-03805129

<https://hal.science/hal-03805129v1>

Submitted on 14 Oct 2023

HAL is a multi-disciplinary open access archive for the deposit and dissemination of scientific research documents, whether they are published or not. The documents may come from teaching and research institutions in France or abroad, or from public or private research centers.

L'archive ouverte pluridisciplinaire **HAL**, est destinée au dépôt et à la diffusion de documents scientifiques de niveau recherche, publiés ou non, émanant des établissements d'enseignement et de recherche français ou étrangers, des laboratoires publics ou privés.



HAL Authorization

1 **Characterization of tuna dark muscle protein isolate**

2

3 **Trong Bach Nguyen^{1*}, Laurine Mule Mueni¹, Tran Nu Thanh Viet Bui¹, Huynh Nguyen Duy**
4 **Bao¹, Nguyen Thi Kim Cuc², Taco Nicolai³**

5

6 ¹Faculty of Food Technology, Nha Trang University, No 2 Nguyen Dinh Chieu, Nha Trang 57000,
7 Vietnam

8 ²Institute of Biotechnology and Environment, Nha Trang University, No 2 Nguyen Dinh Chieu,
9 Nha Trang 57000, Vietnam

10 ³Le Mans Université, IMMM UMR-CNRS 6283, 72085 Le Mans Cedex 9, France

11

12 ***Correspondence**

13 Trong Bach Nguyen, Faculty of Food Technology, Nha Trang University, No 2 Nguyen Dinh
14 Chieu, Nha Trang 57000, Vietnam

15 E-mail: ntbachnt@ntu.edu.vn

16

17 **Abstract**

18 Fish protein isolate (FPI) was extracted from tuna dark muscle (TDM) using the pH-shift method
19 that improves significantly its sensory quality and nutritional value. The amino-acid composition of
20 the FPI was close to that of TDM, but the total protein content was higher. The solubility of FPI in
21 water was higher than 85% at $\text{pH} \geq 6$ and $\text{pH} \leq 3$, but it dropped to about 10% at pH values close to
22 the isoelectric point $\text{pI} \approx 5.0$. The soluble FPI was present in the form of aggregates that were
23 characterized by light-scattering. The microstructure of FPI solutions on larger length scales was
24 probed by confocal microscopy, large protein flocs formed at pH close to pI. SDS-PAGE indicated
25 that a significant fraction of myosin heavy chains was broken down into smaller chains. The

26 viscosity decreased with decreasing of pH, which correlated with the decreasing size of the
27 aggregates.

28

29 **Keywords:** tuna, dark muscle, fish protein isolate, extraction, aggregation

30

31 **Practical application**

32 Tuna dark muscle (TDM) represents a significant fraction of industrially processed tuna. It is
33 currently considered a low value by-product, because it has poor sensory qualities. However, TDM
34 has a high protein content that does not suffer from sensory defects if it is extracted using the pH-
35 shift method. TDM protein isolate therefore has the potential to be a valuable nutritious food
36 ingredient. In order to develop industrial food products with this fish protein isolate it is necessary
37 to characterize it thoroughly.

38

39 **1 INTRODUCTION**

40 Proteins can be effectively isolated from fish by-products by dissolving the proteins at high
41 or low pH and subsequently precipitating them at intermediate pH where the net charge of the
42 proteins is close to zero (Tang et al., 2020). Fish protein isolate (FPI) obtained in this manner can be
43 used as nutritious ingredients in industrial food products (Tang et al., 2020; Desai et al., 2019 &
44 2021; Asad Nawaz et al., 2020). Naturally, in order to optimize the usage of FPI for different types
45 of applications, it is necessary to thoroughly characterize its properties in aqueous solution at
46 different pH.

47 In industrial processing of tuna fish 50-70% of its body mass is considered as by-products
48 (head, skin, dark meat, viscera, bone, etc) of which about 12% is dark muscle (Guérard et al., 2002;
49 Herpandi et al., 2011). It has low commercial value, but is rich in nutrients and its extracted protein
50 displays important technological properties (Sánchez-Zapata et al., 2011). Tuna dark muscle (TDM)
51 contains approximately 27% protein with high nutritional value, but it also contains hemoglobin and

52 myoglobin that can oxidize and thereby render the muscle dark (Chaijan et al., 2010; Ochoa et al.,
53 2017; Tahergorabi et al., 2015; Tian et al., 2017). In recent years, protein recovery from fish dark
54 muscle has attracted the interest of both scientists and manufacturers as it contributes to improved
55 economic efficiency and towards zero-waste processing. In which the recovery method and
56 characterization of protein are the main concerns.

57 The amount of protein that is dissolved from fish muscle depends strongly on the pH
58 (Batista, 1999; Geirsdottir et al., 2007). It was found that at $\text{pH} > 10$ or $\text{pH} < 3.5$ more than 80% of
59 the proteins is soluble, whereas at pH close to the $\text{pI} \approx 5.2\text{-}5.5$ it is less than 10% (Kristinsson et al.,
60 2013). Therefore an efficient method to extract fish protein is to solubilize fish meat in a strong base
61 or acid and subsequently to precipitate the proteins close to pI (Davenport & Kristinsson, 2011; Foh
62 et al., 2012; Y. Kim et al., 2003; Lee et al., 2016; Surasani, 2018; Surasani et al., 2018; Surasani et
63 al., 2016; Undeland et al., 2002; Zhong et al., 2015)(Zhen-Xing Tang et al., 2020). This method
64 removes the dark color and the lipids (Chaijan et al., 2010; Sánchez-Zapata et al., 2011) resulting in
65 a fish protein isolate (FPI) that is useful for food applications. Fish muscle can be dissolved both in
66 strong acid and base, but alkali treatment has advantages in terms of the yield and the strength of
67 gels formed by aqueous FPI solutions (Abdollahi & Undeland, 2018; Batista, 1999; Chaijan et al.,
68 2010; Davenport & Kristinsson, 2011; Kaewdang et al., 2016; Y. Kim et al., 2003; Oliyaei et al.,
69 2016; Zhong et al., 2015).

70 The molecular weight of the protein components of FPI and its distribution have been
71 determined by electrophoresis (Brenner et al., 2009a; Foh et al., 2012; Geirsdottir et al., 2007;
72 Kristinsson & Ingadottir, 2006; Sun et al., 2019; Tian et al., 2017; Yongsawatdigul & Park, 2004).
73 The results show prominent bands corresponding to myosin heavy (≈ 200 kDa) and light (17-23 kD)
74 chains, actin (≈ 43 kDa) and tropomyosin (≈ 38 kDa). The secondary structure of tilapia protein
75 isolate (TPI) was characterized by Kobayashi et al. (2017) using Fourier Transform Infrared
76 spectroscopy (FT-IR). The presence of α -helical and β -sheet structures was demonstrated by
77 absorption bands near 1648 cm^{-1} and 1660 cm^{-1} .

78 Brenner et al. (2009b) characterized FPI extracted from cod in dilute aqueous solutions at
79 pH 11 using light scattering techniques. They found that the protein was present in the form of
80 aggregates with a z-average radius of gyration $R_g = 150$ nm and a hydrodynamic radius $R_h = 180$
81 nm. The FPI also contained about 15 wt% much larger aggregates. The dependence of the scattering
82 intensity on the scattering wave vector showed that the aggregates had a self-similar structure
83 characterized by a fractal dimension of 1.8.

84 The viscosity of FPI in aqueous solution was investigated by Foh et al., (2012) and
85 Geirsdottir et al. (2007). Geirsdottir et al. (2007) observed that the viscosity of herring protein
86 isolate suspensions increased at pH values far from the pI. Foh et al. (2012) found that at pH 7 the
87 viscosity of tilapia protein isolate increased with increasing protein concentration. Brenner et al.
88 (2009a) reported that reduction of the pH from 11 to between 9.5 and 8.5 led to formation of
89 homogeneous gels, whereas reduction to lower pH values down to 3.8 led to formation of
90 heterogeneous gels showing syneresis.

91 It is clear from this brief review that FPI extracted from white flesh and mixed fish by-
92 products has already been studied quite extensively. However, FPI from dark tuna muscle has been
93 rarely investigated. Sánchez-Zapata et al. (2011) reported on the iron and myoglobin content of tuna
94 dark muscle as well as the water and oil holding capacity. Here we present an investigation of the
95 amino acid composition, structure, solubility, and physico-chemical properties of FPI extracted
96 from tuna dark muscle at pH 12 as a function of the pH. The objective is to establish if, and to what
97 extent, FPI from tuna dark muscle is different from other types of FPI so as to facilitate its use in
98 food products.

99

100 **2 MATERIALS AND METHODS**

101 **2.1 Materials**

102 The fish protein isolate used for this study was extracted from yellowfin tuna (*Thunnus*
103 *Albacares*) dark muscle provided by Hai Vuong Co., LTD (Khanh Hoa province, Vietnam) using

104 the alkaline extraction method described by Undeland et al. (2002) with slight modifications. Milled
105 dark muscle was washed twice with deionized water (3:1 ratio) at 4 °C to remove the dark color.
106 Excess water was removed by wrapping the muscle in a filter bag with a pore size of 50 µm and
107 manually pressed. The cleaned muscle was solubilized by adding water at pH 12 at a ratio 1:5. The
108 mixture was homogenized at 4 °C for 2 min at a speed of 3500 rpm using an Ultra-turrax (model:
109 IKA T18, Germany). 2 N NaOH was used to adjust to pH 12 after homogenization. The mixture
110 was stirred for 3 hours at room temperature (20 °C) using an Orbital shaker (model: NB-101M,
111 Korea) and subsequently centrifuged (MF600, Labkorea) at 5000 rpm for 30 min at 4 °C. The
112 supernatant was decanted through a filter bag with a pore-size of 5 µm and the soluble protein was
113 precipitated by reducing the pH to 5.5 using 2 N HCl. The precipitate was thoroughly washed with
114 distilled water at 4 °C. Excess water was removed by manually wrapping and squeezing the protein
115 isolate in a filter bag with a pore size of 5 µm. Finally, the FPI was freeze dried (Lyobeta 35, Spain)
116 and stored at -20 °C. The chemical composition of FPI and TDM is shown in Table 1.

117

118 **2.2 Sample preparation**

119 Stock solutions of FPI were prepared by dissolving the freeze-dried FPI at a concentration of
120 30 g/L in deionized water at pH 12 by stirring for a few hours at ambient temperature. Solutions at
121 lower concentrations and lower pH were prepared by dilution with deionized water and addition of
122 small amounts of 0.1 N HCl.

123

124 **2.3 Methods**

125 **2.3.1 Proximate composition**

126 The composition of tuna dark muscle (TDM) and protein isolate (FPI) extracted from TDM
127 was determined using the procedures of the AOAC (2012). The crude protein content, moisture
128 content, crude fat and ash were determined using the Kjeldahl method, method 928.08, method
129 948.04 and method 920.153, respectively.

130 Sodium, NaCl, and histamine contents were determined using methods 969.23, 930.23, 997.13
131 (LOD = 3 ppm), respectively. Heavy metal (As, Hg, Pb, and Cd) contents were determined using
132 methods 986.15, 971.21, 972.23, and 973.34, respectively.

133

134 ***2.3.2 Fourier Transform Infrared (FT-IR) Spectroscopy***

135 FPI powder was characterized using a FT-IR spectrometer (Model Alpha, Bruker, Ettlingen,
136 Germany) equipped with a horizontal attenuated total reflectance (HATR) accessory. The internal
137 reflection crystal was made of zinc selenide, and had a 45° angle of incidence to the IR beam. The
138 sample was mixed with KBr in the ratio of 98:2 (w/w). A total of 32 scans were done in the
139 wavenumber range from 500 to 4000 cm⁻¹ with a resolution of 4 cm⁻¹. The spectra were collected at
140 room temperature (20 °C) using approximately 0.5 g of the sample that was placed on the surface of
141 the HATR crystal. Analysis of the spectra was carried out using the OPUS 7.0 data collection
142 software program.

143

144 ***2.3.3 Amino acid composition***

145 The amino acid composition of the samples was determined using the method ISO 13903
146 (2005). In brief, FPI samples were hydrolyzed for 24 hours in 6 N HCl at 110 °C in a sealed vessel.
147 The samples were then dissolved in deionized water and filtered. About 20 µL hydrolyzed sample
148 or the standard was injected into the amino acid analyzer (Biochrom 30+, Biochrom Ltd.,
149 Cambridge, UK) equipped with a high pressure PEEK column (No: H-0563) packed with Ultropac
150 8 cation exchange resin (No: 132-56). The automated analyzer was configured with post-column
151 ninhydrin derivatization. The ninhydrin derivative of Pro was detected at 440 nm whereas the
152 remaining amino acid derivatives were detected at 570 nm.

153

154 ***2.3.4 Zeta potential***

155 The zeta potential (ζ) of aqueous FPI solutions at 0.1 g/L was determined as a function of the
 156 pH by measuring the electrophoretic mobility (U_E) using a zeta potential analyser (Nano Partica SZ-
 157 100Z, Horiba Scientific, Japan). The zeta potential was calculated from the electrophoretic mobility
 158 by applying Henry's equation (Lunardi et al., 2021):

$$159 \quad U_E = \frac{2\varepsilon \cdot \zeta \cdot f(\kappa\alpha)}{3\eta} \quad (1)$$

160 where, ε is the permittivity, $f(\kappa\alpha)$ is the Henry coefficient and η is the dispersion viscosity.
 161 Following the Smoluchowski approximation $f(\kappa\alpha)$ was set at 1.5. All measurements were done in
 162 triplicate.

163

164 **2.3.5 Light scattering**

165 Dynamic and static light scattering measurements were conducted with a commercial
 166 apparatus (ALV-CGS3, ALV-Langen) operating with a vertically polarized He-Ne laser with
 167 wavelength $\lambda = 632$ nm. The temperature was controlled at 20 °C with a thermostat bath to within \pm
 168 0.2 °C. The measurements were performed on FPI solutions diluted to below 1 g/L in order to avoid
 169 the effect of interactions and at angles of observation between 13° and 140°. The relative scattering
 170 intensity (I_r), of the solute, calculated as the intensity minus the solvent scattering divided by the
 171 scattering intensity of toluene, is related to the weight average molar mass (M_w) and the scattering
 172 wave vector (q) dependent structure factor ($S(q)$) (Brown, 1993):

$$173 \quad \frac{I_r}{KC} = M_w S(q) \quad (2)$$

174 where K is an optical constant defined as:

$$175 \quad K = \frac{4\pi^2 n_s^2}{\lambda^4 N_A} \left(\frac{\partial n}{\partial C} \right)^2 \left(\frac{n_{tol}}{n_s} \right)^2 \frac{1}{R_{tol}} \quad (3)$$

176 with N_A is Avogadro's number, $\partial n/\partial C = 0.189$ mL/g the refractive index increment and $R_{tol} = 1.35$
 177 $\times 10^{-5}$ 1/cm the Rayleigh constant of toluene at 20 °C.

178 The normalized electric field autocorrelation functions ($g_1(t)$) obtained from dynamic light
179 scattering measurements (Berne & Pecora, 1976) were analyzed in terms of a distribution of
180 relaxation times (τ):

$$181 \quad g_1(t) = \int A(\tau) \exp(-t/\tau) d(\tau) \quad (4)$$

182 In dilute solution, the relaxation was caused by translational diffusion of the particles. The diffusion
183 coefficient (D) was calculated from the average relaxation rate:

$$184 \quad D = \langle \tau^{-1} \rangle / q^2 \quad (5)$$

185 The z-average hydrodynamic radius (R_h) of the solute was calculated from D extrapolated to $q = 0$
186 using the Stokes-Einstein equation:

$$187 \quad R_h = \frac{kT}{6\pi\eta D} \quad (6)$$

188 with η the viscosity of the solvent, k Boltzman's constant, and T the absolute temperature.

189

190 ***2.3.6 Confocal Laser Scanning Microscopy***

191 The morphology of FPI solutions was studied with Confocal Laser Scanning Microscopy
192 (CLSM) in the fluorescence with mode utilizing a Zeiss LSM 800 microscope (Oberkochen,
193 Germany). A water immersion objective lens was used (HCxPL APO 63x NA=1.2 with a
194 theoretical resolution of 0.1 μm in the x-y plane. The proteins were fluorescently labeled by adding
195 5 ppm rhodamine B that physically bound to the proteins. No effect of labeling was observed at the
196 concentration used. The fluorescent label was excited by a laser at 543 nm and the fluorescent light
197 was detected between 543 and 900 nm. The solutions were inserted between a concave slide and a
198 coverslip and hermetically sealed.

199

200 ***2.3.7 Viscosity measurement***

201 The viscosity was measured at 20 °C as a function of the shear rate using a rheometer
202 (Kinexus Pro 50N, Malvern, England) with a cone and plate geometry (diameter 60 mm; angle 1°).

203 After loading, the samples were pre-sheared at 100 s^{-1} for 1 min. The viscosity was determined as a
204 function of the shear rate between $0.1\text{-}1000 \text{ s}^{-1}$.

205

206 ***2.3.8 Sodium dodecyl sulphate–polyacrylamide gel electrophoresis (SDS-PAGE)***

207 FPI solutions at 5 g/L and different pH were mixed with the same volume of an
208 electrophoresis sample buffer (0.25 M Tris (pH 6.8), 2% SDS, 10% glycerol, 100 mM
209 dithiothreitol, 0.2% bromophenol blue) and heated at $95 \text{ }^\circ\text{C}$ for 10 min. The running gel contained
210 15% polyacrylamide in 0.5 M Tris–HCl (pH 8.8) and 0.3% SDS, whereas the stacking gel
211 contained 5% polyacrylamide in 0.5 M Tris HCl (pH 6.8) and 0.2% SDS. The electrode buffer
212 contained 0.025 mol/L Tris– HCl, 0.192 M glycine and 0.1% SDS at pH 8.3. SDS-PAGE
213 electrophoresis was performed at 15 mA using a Mini Protean II unit (Bio-Rad Laboratories, Inc.,
214 Richmond, CA, USA). Following electrophoresis, the gels were stained with 0.05% Coomassie
215 Blue G250 in 25% v/v ethanol and 10% v/v acetic acid for 4 h. The gel was finally destained with
216 an aqueous solution containing 5% (v/v) methanol and 10% (v/v) acetic acid. Molecular weights of
217 the FPI subunits were estimated using molecular weight standards (Invitrogen, USA) in the range
218 from 3.5 kDa to 260 kDa.

219

220 ***2.3.9 Solubility***

221 Protein solutions at 10 g/L and different pH were centrifuged at $1.3 \times 10^4 \text{g}$ for 30 min at 20
222 $^\circ\text{C}$ by a refrigerated centrifuge (Hettich, Mikro 22R, Germany). The protein concentration of the
223 supernatant was determined by UV absorption at 278 nm with a UV-Visible spectrometer (Libra
224 S50 Bio, Cambridge, England) using an extinction coefficient 1.0 L/g.cm . The soluble protein
225 fraction was determined by dividing the protein concentration in the supernatant by the total
226 concentration. All measurements were done in triplicate.

227

228 **2.4 Statistical analysis**

229 Statistical analysis of the data was performed using SPSS software (Version 16.0, Chicago,
230 IL, USA). One-way analysis of variance (ANOVA) by the Student's T-test was used for statistical
231 comparisons of means. Standard deviations and differences at $P < 0.05$ are indicated.

232

233 **3 RESULTS AND DISCUSSION**

234 **3.1 FPI powder characterization**

235 *3.1.1 Amino acid composition*

236 The amino acid composition of tuna dark muscle and fish protein isolate extracted from
237 TDM is given in Table 2. As expected, the total protein content in FPI was higher (90%) than in
238 TDM (73%), but the amino acid composition of the proteins was similar with glutamic acid,
239 aspartic acid, leucine, and lysine as the most abundant amino acids. The fraction of essential amino
240 acids (EAA) was 44% in TMA and 45% in FPI. The amino acid composition was similar to that
241 reported for muscle tissue of yellowfin tuna by Peng et al. (2013) and for FPI extracted from pangas
242 (*Pangasius pangasius*) processing waste (Surasani et al., 2018).

243

244 *3.1.2 Fourier-Transform Infrared Spectroscopy*

245 As far as we are aware, the only previous FT-IR study of FPI was reported by Kobayashi et
246 al. (2017) for tilapia protein isolate. These authors focused on the amide I ($1600 - 1700 \text{ cm}^{-1}$) and
247 amide II ($1500\text{--}1600 \text{ cm}^{-1}$) regions. They assigned the amide I band with a maximum at 1639 cm^{-1}
248 to the β -sheet structure and the amide II with a maximum at 1550 cm^{-1} to the α -helix structure.
249 Figure 1 compares the FT-IR spectra of TDM and the FPI powder. Small, but significant
250 differences were observed indicating that the extraction procedure had some influence on the
251 secondary structure of the proteins. The height of the amide II band relative to the amide I band was
252 lower for FPI and a shoulder appeared around 1740 cm^{-1} , indicating that FPI contained relatively
253 less α -helices. The amide II peak for FPI from tuna was higher than for FPI paste from talapia
254 reported by Kobayashi et al., (2017). The higher α -helix content was perhaps caused by the high

255 concentrations of amino acids (alanine, glutamic acid, lysine and leucine), which generally prefer to
256 adopt an α -helix structure. However, one needs to be careful when comparing these results directly,
257 because the FPI paste investigated by Kobayashi et al. (2017) contained 75% water, whereas the
258 FPI powder studied here contained very little water.

259

260 **3.2 Characterization of tuna dark muscle protein isolate solutions at different pH**

261 **3.2.1 Zeta-potential**

262 The zeta potential (ζ) of FPI as a function of the pH is shown in figure 2. It changed from
263 strongly positive at $\text{pH} < 4$ to strongly negative at $\text{pH} \geq 6$. The isoelectric point (pI) was close to pH
264 5.

265

266 **3.2.2 Solubility**

267 The solubility of FPI in water was determined as a function of the pH between 2 and 12.
268 Figure 3 shows that FPI solutions were transparent between pH 6 and pH 12, but became
269 increasingly turbid at lower pH down to pH 5.0 indicating the formation more and larger
270 aggregates. At pH 5.0 a dense precipitate was formed. Protein aggregates also precipitated at pH 4,
271 but the precipitate was less dense. With further decrease of the pH the turbidity decreased indicating
272 that fewer and smaller aggregates were formed.

273 The fraction of soluble proteins (F_{pis}) was determined by measuring the protein
274 concentration of the supernatant after centrifugation as described in the section 2.3.9, see figure 4.
275 At $\text{pH} \geq 6.0$ and $\text{pH} \leq 3.0$, F_{pis} was higher than 0.85, but close to the pI, F_{pis} decreased to values as
276 low as 0.12. These results are similar to those reported by Foh et al. (2012) for tilapia protein isolate
277 and Sun et al. (2019) for myosin extracted from skeletal muscle of blue round scads. Similar
278 observations were also reported for white muscle from cod, rockfish and Alaska pollock (Brenner et
279 al., 2009a; Y. S. Kim & Park, 2008; Yongsawatdigul & Park, 2004). The low solubility close to pI
280 can be attributed to weak electrostatic repulsions between the proteins.

281

282 **3.2.3 SDS analysis**

283 The protein composition of soluble FPI was analyzed by SDS-PAGE at different pH above
284 pH 6 and below pH 3. The results show numerous bands spread out over the whole range of
285 molecular weights from 15 kDa to 260 kDa independent of the pH, see figure 5. The distinct band at
286 15 kDa can be attributed to myosin light chains. Indistinct bands at 37 kDa and 42 kDa correspond
287 to tropomyosin and actin, respectively (Abdollahi & Undeland, 2018; Taktak et al., 2018).
288 However, albumins (from the sarcoplasmic fraction) are also typically found in this region (Felix et
289 al., 2017). Remarkably no distinct band corresponding to myosin heavy chains (MHC) was
290 observed at 250 kDa. This could indicate that polymerization of MHC had occurred resulting in
291 larger proteins that could not enter the gel (Y. S. Kim & Park, 2008; Nunez-Flores et al., 2018).
292 Alternatively, the absence was caused by a high degree of hydrolysis due to the well-known high
293 proteolytic enzyme activity in the dark muscle (Abdollahi & Undeland, 2018; Kristinsson &
294 Ingadottir, 2006; Zhong et al., 2015), which would explain the presence of proteins with an almost
295 continuous range of lower molecular weights.

296

297 **3.2.4 Size & molar mass**

298 The size and molecular weight of FPI in aqueous solution was determined using static and
299 dynamic light scattering at 20 °C. The z-average hydrodynamic radius (R_h) and weight average
300 molar mass (M_w) were determined as described in section 2.3.5 and are shown as a function of the
301 pH in figure 6. Aggregates with $R_h \approx 230$ nm and $M_w \approx 10^7$ g/mol were formed at the highest pH
302 (11 and 12). The aggregate size and molar mass decreased with decreasing pH down to $R_h \approx 90$ nm
303 and $M_w \approx 1.4 \times 10^6$ g/mol at pH 7-9. At pH 3 the aggregates were again slightly larger than at pH 6,
304 but at pH 2 the size was close to that at pH 7-9. Most FPI precipitated between pH 3 and 6 and
305 could not be analyzed by light scattering. It is curious that the aggregate size increased strongly
306 between pH 9 and pH 11 even though the zeta potential remained approximately constant. As was

307 mentioned in the Introduction, Brenner et al. (2009b) observed $R_h = 180$ nm for FPI extracted from
308 cod at pH 11.

309

310 **3.2.5 Microstructure**

311 The microstructure of FPI at 10 g/L was investigated with CLSM at different pH, see figure
312 7. Between pH 12 and pH 5.8, where the solutions were transparent, the CLSM images were
313 homogeneous showing only a few microscopic particles. Significantly more microscopic particles
314 were seen at pH 5.7 and at lower pH down to pH 3.5 larger protein flocs were formed (Figure 7). At
315 pH 3 and lower the images were again homogeneous (not shown). The larger flocs sedimented
316 during centrifugation and at some pH values even under gravity as was shown in section 3.2.2.

317

318 **3.2.6 Viscosity**

319 The viscosity of FPI solutions at 10 g/L at different pH was measured as a function of the
320 shear rate, see figure 8. Significant shear thinning was observed at all pH values. At a given shear
321 rate the viscosity was highest at the highest pH values (11 and 12) and decreased strongly with
322 decreasing pH down to pH 6. At pH 3 the viscosity was again higher, but at pH 2 it was close to that
323 in the pH range 6-9. Comparison with the results on the aggregate size shown in section 3.2.4 shows
324 the pH dependence of the viscosity was correlated with that of the average aggregate size - FPI
325 solutions containing larger aggregates being more viscous. The effect of the concentration of FPI
326 solutions is shown in Figure 9 at pH 2 and pH 12. As expected, the viscosity increased with
327 increasing in protein concentration. The increase was more important for the solution at pH 12 that
328 contained larger aggregates. These results can be explained by the fact that larger aggregates take
329 up a larger volume fraction as has been discussed in more detail for whey protein aggregates by
330 Inthavong et al. (2019).

331

332 **4 CONCLUSIONS**

333 FPI can be extracted from tuna dark muscle using the pH-shift method. The FPI was rich in
334 essential amino acids and kept the secondary structure of raw material. More than 85% of the FPI
335 proteins could be solubilized at $\text{pH} \geq 6$ and $\text{pH} \leq 3$ in the form of aggregates that were significantly
336 larger at pH 10 and 12 than between pH 6 and 9 and below pH 3. At intermediate pH FPI formed
337 large flocs that sedimented under gravity. Soluble FPI solutions were shear thinning with a viscosity
338 that was increased strongly for $\text{pH} \geq 10$ where the solutions contained larger aggregates. A
339 significant fraction of the myosin heavy chains was broken down into smaller chains. The FPI
340 extracted in this manner has an excellent potential for application in food products for human
341 consumption.

342

343 **ACKNOWLEDGEMENTS**

344 This research is funded by Vietnam National Foundation for Science and Technology Development
345 (NAFOSTED) under grant number 106.99-2018.42.

346 Authors also authenticate the co-collaborations of the Center of Analytical Services and
347 Experimentation of Ho Chi Minh City (HCMC, Vietnam) for amino acid analysis. And we are also
348 grateful to Prof. Christophe Chassenieux, Prof. Lazhar Benyahia and Dr. Frédéric Renou at IMMM
349 (Le Mans, France) for the valuable discussions.

350 Many thanks to Nguyen Thi Anh Ky and Tran Thi Hong Van for their assistance in sample
351 preparations.

352

353 **DATA AVAILABILITY STATEMENT**

354 The data that support the findings of this study are available from the corresponding author upon
355 request.

356

357 **CONFLICTS OF INTEREST**

358 The authors declared no conflicts of interest.

359

360 **ORCID**

361 Trong Bach Nguyen: <https://orcid.org/0000-0001-7426-3418>

362 Huynh Nguyen Duy Bao: <https://orcid.org/0000-0003-4158-5343>

363 Taco Nicolai: <https://orcid.org/0000-0002-7206-1975>

364

365 **REFERENCES**

366 Abdollahi, M., & Undeland, I. (2018). Structural, functional, and sensorial properties of protein
367 isolate produced from salmon, cod, and herring by-products. *Food and Bioprocess*
368 *Technology, 11*, 1733-1749.

369 AOAC. (2012). Official methods of analysis of AOAC International (19th ed.). *Association of*
370 *Official Analytical Chemists, Washington, DC.*

371 Batista, I. (1999). Recovery of proteins from fish waste products by alkaline extraction. *European*
372 *Food Research and Technology, 210*, 84-89.

373 Berne, J. B., & Pecora, R. (1976). *Laser Spectroscopy: Dynamic Light Scattering. With*
374 *Applications to Chemistry, Biology, and Physics.* Wiley-Interscience, New York, 1976. viii,
375 376 pp.,. *Science, 194*, 1155-1156.

376 Brenner, T., Johannsson, R., & Nicolai, T. (2009a). Characterisation and thermo-reversible gelation
377 of cod muscle protein isolates. *Food Chemistry, 115*, 26-31.

378 Brenner, T., Johannsson, R., & Nicolai, T. (2009b). Characterization of fish myosin aggregates
379 using static and dynamic light scattering. *Food Hydrocolloids, 23*, 296-305.

380 Brown, W. 1993. *Dynamic light scattering: the method and some applications* (Vol. 49): Clarendon
381 Press.

382 Chaijan, M., Panpipat, W., & Benjakul, S. (2010). Physicochemical and gelling properties of short-
383 bodied mackerel (*Rastrelliger brachysoma*) protein isolate prepared using alkaline-aided
384 process. *Food and Bioproducts Processing, 88*, 174-180.

385 Davenport, M. P., & Kristinsson, H. G. (2011). Channel catfish (*Ictalurus punctatus*) muscle protein
386 isolate performance processed under different acid and alkali pH values. *Journal of Food*
387 *Science*, 76, E240-247.

388 Felix, M., Romero, A., Rustad, T., & Guerrero, A. (2017). Physicochemical, microstructure and
389 bioactive characterization of gels made from crayfish protein. *Food Hydrocolloids*, 63, 429-
390 436.

391 Foh, M. K., Wenshui, X., Amadou, I., & Jiang, Q. (2012). Influence of pH shift on functional
392 properties of protein isolated of tilapia (*Oreochromis niloticus*) muscles and of soy protein
393 isolate. *Food and Bioprocess Technology*, 5, 2192-2200.

394 Geirsdottir, M., Hlynsdottir, H., Thorkelsson, G., & Sigurgisladottir, S. (2007). Solubility and
395 viscosity of herring (*Clupea harengus*) proteins as affected by freezing and frozen storage.
396 *Journal of Food Science*, 72, C376-380.

397 Guérard, F., Guimas, L., & Binet, A. (2002). Production of tuna waste hydrolysates by a
398 commercial neutral protease preparation. *Journal of molecular catalysis B: Enzymatic*, 19,
399 489-498.

400 Herpandi, N. H., Rosma, A., & Wan Nadiah, W. (2011). The tuna fishing industry: A new outlook
401 on fish protein hydrolysates. *Comprehensive Reviews in Food Science and Food Safety*, 10,
402 195-207.

403 Inthavong, W., Chassenieux, C., & Nicolai, T. (2019). Viscosity of mixtures of protein aggregates
404 with different sizes and morphologies. *Soft Matter*, 15, 4682-4688.

405 ISO. (2005). Animal feeding stuffs – Determination of amino acids content.

406 Kaewdang, O., Benjakul, S., Prodpran, T., Kaewmanee, T., & Kishimura, H. (2016). Characteristics
407 of Gelatin Extracted from the Swim Bladder of Yellowfin Tuna (*Thunnus albacores*) as
408 Affected by Alkaline Pretreatments. *Journal of Aquatic Food Product Technology*, 25,
409 1190-1201.

410 Kim, Y., Park, J. W., & Choi, Y. (2003). New approaches for the effective recovery of fish proteins
411 and their physicochemical characteristics. *Fisheries Science*, 69, 1231-1239.

412 Kim, Y. S., & Park, J. W. (2008). Negative roles of salt in gelation properties of fish protein isolate.
413 *Journal of Food Science*, 73, C585-588.

414 Kobayashi, Y., Mayer, S. G., & Park, J. W. (2017). FT-IR and Raman spectroscopies determine
415 structural changes of tilapia fish protein isolate and surimi under different comminution
416 conditions. *Food Chemistry*, 226, 156-164.

417 Kristinsson, H. G., & Ingadottir, B. (2006). Recovery and properties of muscle proteins extracted
418 from tilapia (*Oreochromis niloticus*) light muscle by pH shift processing. *Journal of Food*
419 *Science*, 71, E132-E141.

420 Kristinsson, H. G., Lanier, T. C., Halldorsdottir, S. M., Geirsdottir, M., & Park, J. W. (2013). Fish
421 protein isolate by pH shift. *Surimi and surimi seafood*, 169-192.

422 Laemmli, U. K. (1970). Cleavage of structural proteins during the assembly of the head of
423 bacteriophage T4. *nature*, 227, 680-685.

424 Lee, H. J., Lee, G. W., Yoon, I. S., Park, S. H., Park, S. Y., Kim, J. S., & Heu, M. S. (2016).
425 Preparation and characterization of protein isolate from Yellowfin tuna *Thunnus albacares*
426 roe by isoelectric solubilization/precipitation process. *Fisheries and Aquatic Sciences*, 19.

427 Lunardi, C. N., Gomes, A. J., Rocha, F. S., De Tommaso, J., & Patience, G. S. (2021).
428 Experimental methods in chemical engineering: Zeta potential. *The Canadian Journal of*
429 *Chemical Engineering*, 99, 627-639.

430 Nunez-Flores, R., Cando, D., Borderias, A. J., & Moreno, H. M. (2018). Importance of salt and
431 temperature in myosin polymerization during surimi gelation. *Food Chem*, 239, 1226-1234.

432 Ochoa, T. J., Baiocchi, N., Valdiviezo, G., Bullon, V., Campos, M., & Llanos-Cuentas, A. (2017).
433 Evaluation of the efficacy, safety and acceptability of a fish protein isolate in the nutrition of
434 children under 36 months of age. *Public Health Nutrition*, 20, 2819-2826.

- 435 Oliyaei, N., Ghorbani, M., Moosavi-Nasab, M., Sadeghimahoonak, A. R., & Maghsoudloo, Y.
436 (2016). Effect of Temperature and Alkaline pH on the Physicochemical Properties of the
437 Protein Isolates Extracted from the Whole Ungutted Lanternfish (*Benthoosema pterotum*).
438 *Journal of Aquatic Food Product Technology*, 26, 1134-1143.
- 439 Peng, S., Chen, C., Shi, Z., & Wang, L. (2013). Amino acid and fatty acid composition of the
440 muscle tissue of yellowfin tuna (*Thunnus albacares*) and bigeye tuna (*Thunnus obesus*).
441 *Journal of Food and Nutrition Research*, 1, 42-45.
- 442 Sánchez-Zapata, E., Amensour, M., Oliver, R., Fuentes-Zaragoza, E., Navarro, C., Fernández-
443 López, J., Sendra, E., Sayas, E., & Pérez-Alvarez, J. A. (2011). Quality Characteristics of
444 Dark Muscle from Yellowfin Tuna *Thunnus albacares* to Its Potential Application in the
445 Food Industry. *Food and Nutrition Sciences*, 02, 22-30.
- 446 Sun, L. C., Lin, Y. C., Liu, W. F., Qiu, X. J., Cao, K. Y., Liu, G. M., & Cao, M. J. (2019). Effect of
447 pH shifting on conformation and gelation properties of myosin from skeletal muscle of blue
448 round scads (*Decapterus maruadsi*). *Food Hydrocolloids*, 93, 137-145.
- 449 Surasani, V. K. R. (2018). Acid and alkaline solubilization (pH shift) process: a better approach for
450 the utilization of fish processing waste and by-products. *Environ Sci Pollut Res Int*, 25,
451 18345-18363.
- 452 Surasani, V. K. R., Kudre, T., & Ballari, R. V. (2018). Recovery and characterization of proteins
453 from pangas (*Pangasius pangasius*) processing waste obtained through pH shift processing.
454 *Environ Sci Pollut Res Int*, 25, 11987-11998.
- 455 Surasani, V. K. R., Tyagi, A., & Kudre, T. (2016). Recovery of Proteins from Rohu Processing
456 Waste Using pH Shift Method: Characterization of Isolates. *Journal of Aquatic Food
457 Product Technology*, 26, 356-365.
- 458 Tahergorabi, R., Matak, K. E., & Jaczynski, J. (2015). Fish protein isolate: Development of
459 functional foods with nutraceutical ingredients. *Journal of Functional Foods*, 18, 746-756.

460 Taktak, W., Nasri, R., Hamdi, M., Gomez-Mascaraque, L. G., Lopez-Rubio, A., Li, S., Nasri, M., &
461 Karra-Chaâbouni, M. (2018). Physicochemical, textural, rheological and microstructural
462 properties of protein isolate gels produced from European eel (*Anguilla anguilla*) by heat-
463 induced gelation process. *Food Hydrocolloids*, 82, 278-287.

464 Tian, Y., Wang, W., Yuan, C., Zhang, L., Liu, J., & Liu, J. (2017). Nutritional and Digestive
465 Properties of Protein Isolates Extracted from the Muscle of the Common Carp Using pH-
466 Shift Processing. *Journal of Food Processing and Preservation*, 41, e12847.

467 Undeland, I., Kelleher, S. D., & Hultin, H. O. (2002). Recovery of functional proteins from herring
468 (*Clupea harengus*) light muscle by an acid or alkaline solubilization process. *Journal of*
469 *agricultural and food chemistry*, 50, 7371-7379.

470 Yongsawatdigul, J., & Park, J. W. (2004). Effects of alkali and acid solubilization on gelation
471 characteristics of rockfish muscle proteins. *Journal of food science*, 69, 499-505.

472 Zhong, S., Liu, S., Cao, J., Chen, S., Wang, W., & Qin, X. (2015). Fish Protein Isolates Recovered
473 from Silver Carp (*Hypophthalmichthys molitrix*) By-Products Using Alkaline pH
474 Solubilization and Precipitation. *Journal of Aquatic Food Product Technology*, 25, 400-413.

475

476

477

478

479

480

481

482

483

484

485

486

487

488

TABLE 1 Chemical composition of tuna dark muscle and FPI.

489

PROXIMATE	Unit	TDM	FPI
Moisture content	wt%	69.40 ± 0.66 ^a	77.30 ± 0.87 ^b
Ash	wt%	1.20 ± 0.04 ^a	1.40 ± 0.04 ^b
Protein	wt%	26.30 ± 0.35 ^a	20.10 ± 0.30 ^b
Fat	wt%	2.54 ± 0.09 ^a	0.66 ± 0.06 ^b
Sodium	mg/kg	577.3 ± 2.85 ^a	435.4 ± 2.00 ^b
Histamine	mg/kg	nd	nd
(LOD = 3 ppm)			
NaCl	mg/kg	-	1.09 ± 0.05
Arsenic (As)	mg/kg	-	nd
Mercury (Hg)	mg/kg	-	nd
Lead (Pb)	mg/kg	-	nd
Cadmium (Cd)	mg/kg	-	nd

Note: Different superscript letters within the same row represent significantly different ($P < 0.05$).

Abbreviations: nd (not detected); LOD (Limit of Detection)

490

491

492

493

494

495

496

TABLE 2 Amino acid composition of tuna dark muscle and protein isolate (dry basis).

Amino Acid	TDM (g/100g)	FPI (g/100g)
Alanine (Ala)	5.04 ± 0.30 ^a	5.11 ± 0.62 ^a
Arginine (Arg)	4.21 ± 0.14 ^a	5.63 ± 0.57 ^b
Aspartic acid (Asp)	7.21 ± 0.14 ^a	9.24 ± 0.3 ^b
Glutamic acid (Glu)	11.14 ± 0.68 ^a	16.21 ± 0.63 ^b
Glycine (Gly)	3.70 ± 0.20 ^a	3.38 ± 0.12 ^a
Histidine (His) ^{**}	3.57 ± 0.27 ^a	2.40 ± 0.13 ^b
Isoleucine (Ile) [*]	3.95 ± 0.30 ^a	4.89 ± 0.23 ^b
Leucine (Leu) [*]	6.49 ± 0.24 ^a	8.29 ± 0.35 ^b
Lysine (Lys) [*]	7.77 ± 0.33 ^a	9.42 ± 0.33 ^b
Methionine (Met) [*]	2.07 ± 0.07 ^a	3.00 ± 0.24 ^b
Phenylalanine (Phe) [*]	3.14 ± 0.16 ^a	4.16 ± 0.26 ^b
Proline (Pro)	2.36 ± 0.26 ^a	2.38 ± 0.25 ^a
Serine (Ser)	2.98 ± 0.21 ^a	3.93 ± 0.17 ^b
Threonine (Thr) [*]	3.07 ± 0.12 ^a	4.21 ± 0.15 ^b
Tyrosine (Tyr) [*]	2.60 ± 0.36 ^a	3.26 ± 0.11 ^b
Valine (Val) [*]	3.48 ± 0.35 ^a	5.04 ± 0.22 ^a
EAA	32.56	42.26

TAA**72.79****90.55**

Note: Different superscript letters within the same row represent significantly different ($P < 0.05$).

EAA -total essential amino acid, TAA-total amino acid

* Essential amino acids according to (FAO/WHO, 1975)

** Indispensable amino acid in human adult according to FAO/WHO/UNU (1985)

497

498

499

500

501

502

503

504

505

506

507

508

509

510

511

512

513

514

515

516

517

518

519 **Legend of Figures**

520 **FIGURE 1** Fourier Transform Infrared Spectroscopy spectra of tuna dark muscle and FPI powder at
521 two different ranges of the wave number: 4000-500 cm^{-1} (a) and 2000-1400 cm^{-1} (b).

522 **FIGURE 2** Zeta potential of FPI as a function of pH.

523 **FIGURE 3** Photos of solutions of 10 g/L FPI taken 3 h after setting the pH at different values
524 indicated in the figure.

525 **FIGURE 4** Fraction of proteins in the supernatant as a function of pH for FPI solutions at 10 g/L.

526 **FIGURE 5** SDS-PAGE pattern of FPI at pH 2 (middle) and pH 12 (right). The left column shows
527 distinct bands of the markers with molar masses indicated in the figure.

528 **FIGURE 6** Average hydrodynamic radius (circle) and molar mass (triangle) of aggregates of
529 soluble FPI in aqueous solution at different pH.

530 **FIGURE 7** CLSM images of FPI solutions at 10 g/L at different pH. The images represent 110
531 $\times 110 \mu\text{m}$.

532 **FIGURE 8** pH-dependence of the shear viscosity for FPI solutions at 10 g/L at a shear rate of 1 s^{-1} .

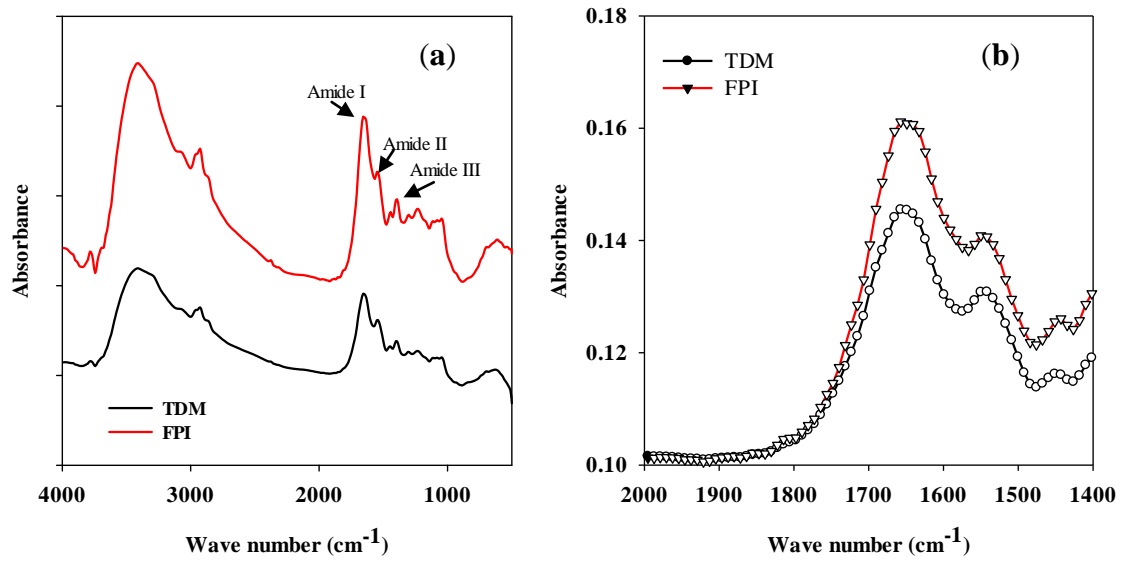
533 **FIGURE 9** Protein concentration dependence of the shear viscosity for FPI solutions at pH 2
534 (circle) and pH 12 (triangle) and at shear rate of 1 s^{-1} . Solid lines are guides to the eye.

535

536

537

538



539

540 **FIGURE 1** Fourier Transform Infrared Spectroscopy spectra of tuna dark muscle and FPI powder at
 541 different range of wave number: 4000-500 cm⁻¹ (a) and 2000-1400 cm⁻¹ (b).

542

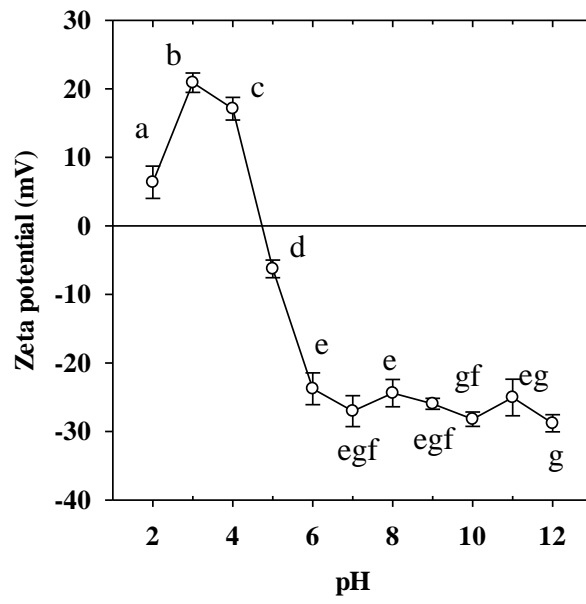
543

544

545

546

547



548

549 **FIGURE 2** Zeta potential of FPI as a function of the pH.

550

551

552

553

554

555

556

557

558

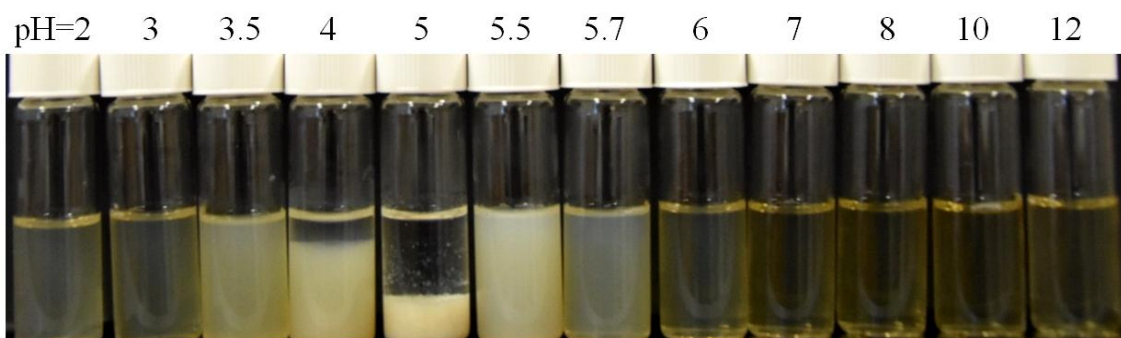
559

560

561

562

563



564

565 **FIGURE 3** Photos of solutions of 10 g/L FPI taken 3 h after setting the pH at different values
566 indicated in the figure.

567

568

569

570

571

572

573

574

575

576

577

578

579

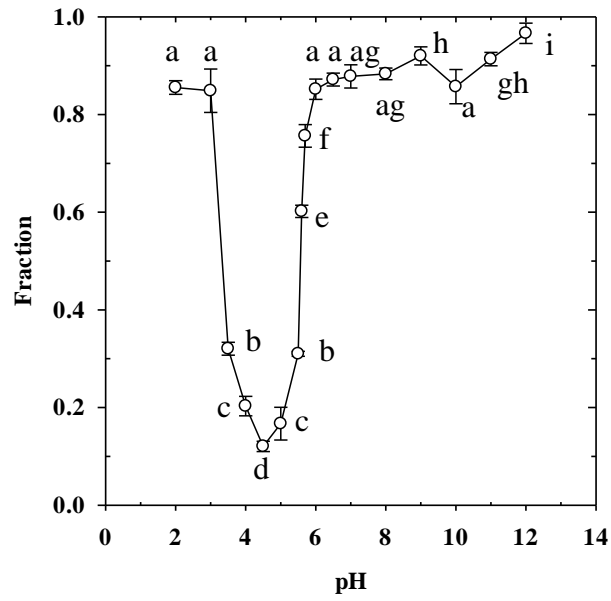
580

581

582

583

584



585

586 **FIGURE 4** Fraction of proteins in the supernatant as a function of pH for FPI solutions at 10 g/L.

587

588

589

590

591

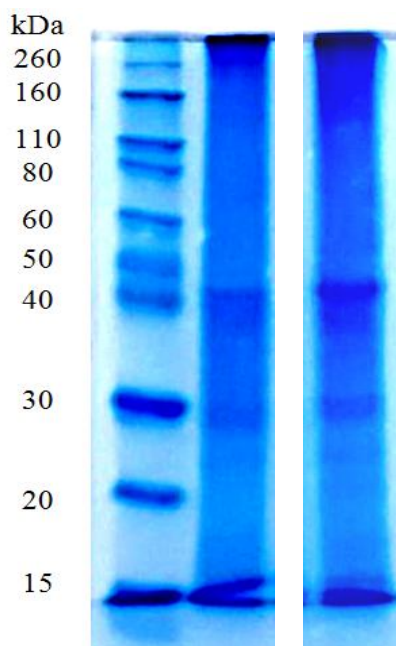
592

593

594

595

596



597 **FIGURE 5** SDS-PAGE pattern of FPI at pH 2 (middle) and pH 12 (right). The left column shows
598 distinct bands of the markers with molar masses indicated in the figure.

599

600

601

602

603

604

605

606

607

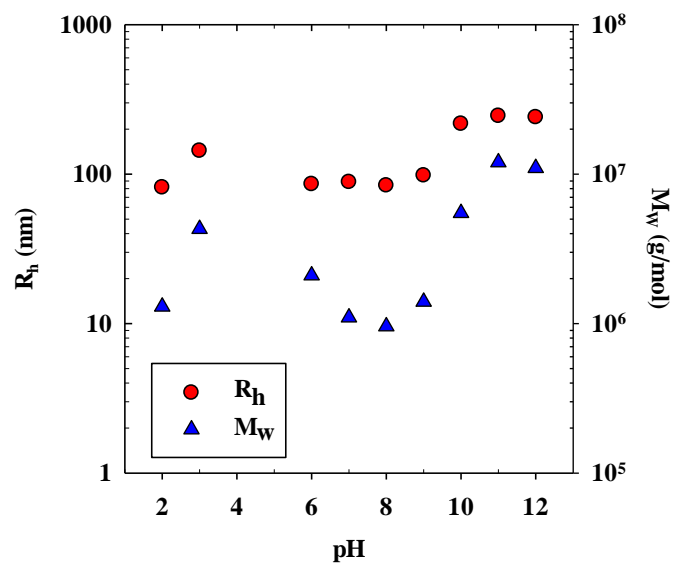
608

609

610

611

612



613

614 **FIGURE 6** Average hydrodynamic radius (circle) and molar mass (triangle) of aggregates of
 615 soluble FPI in aqueous solution at different pH.

616

617

618

619

620

621

622

623

624

625

626

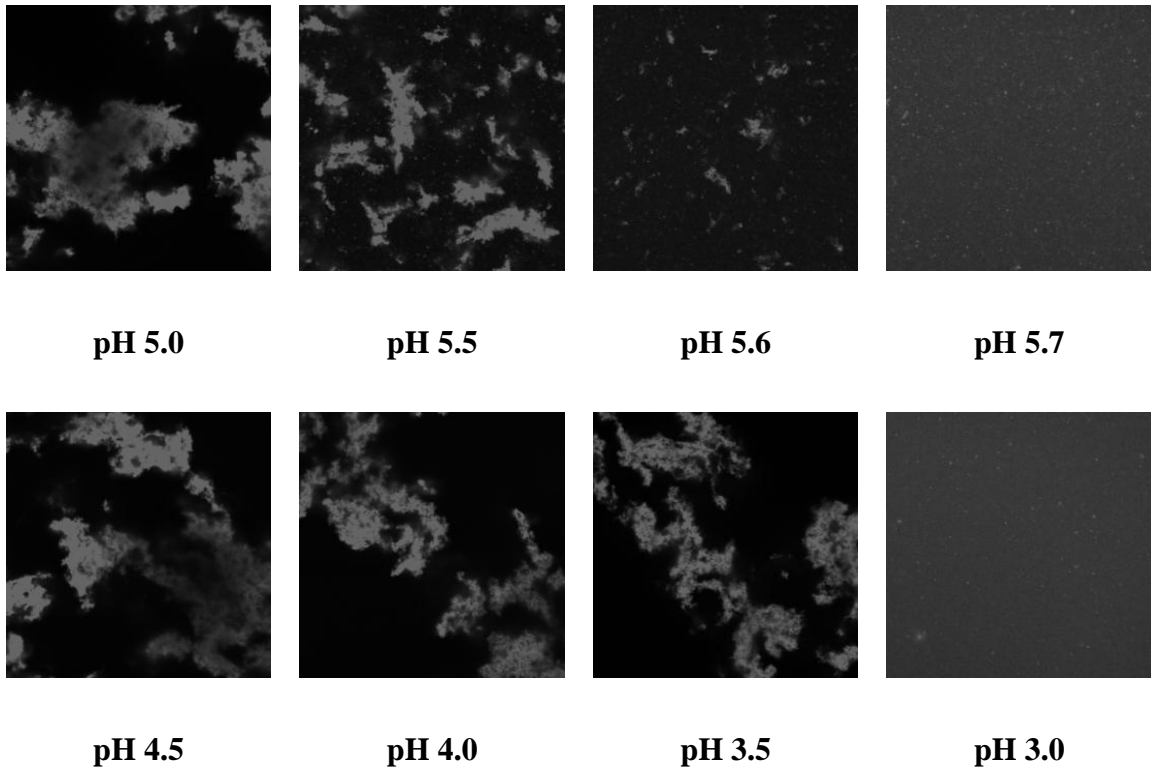
627

628

629

630

631



632 **FIGURE 7** CLSM images of FPI solutions at 10 g/L at different pH. The images represent 110
633 x110 μm .

634

635

636

637

638

639

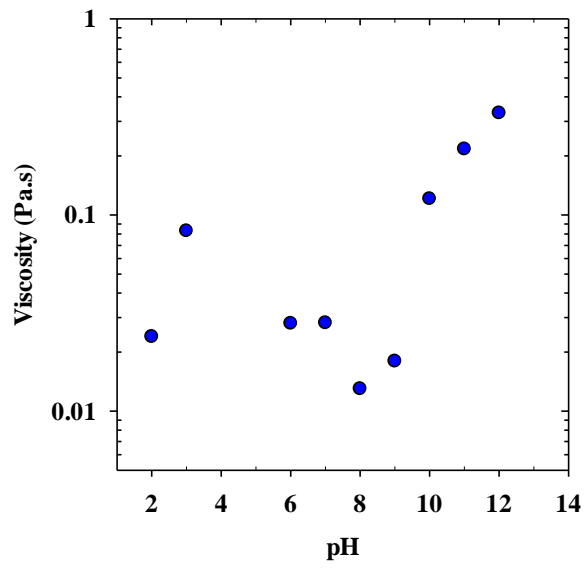
640

641

642

643

644



645

646 **FIGURE 8** pH-dependence of the shear viscosity for FPI solutions at 10 g/L at a shear rate of 1 s^{-1} .

647

648

649

650

651

652

653

654

655

656

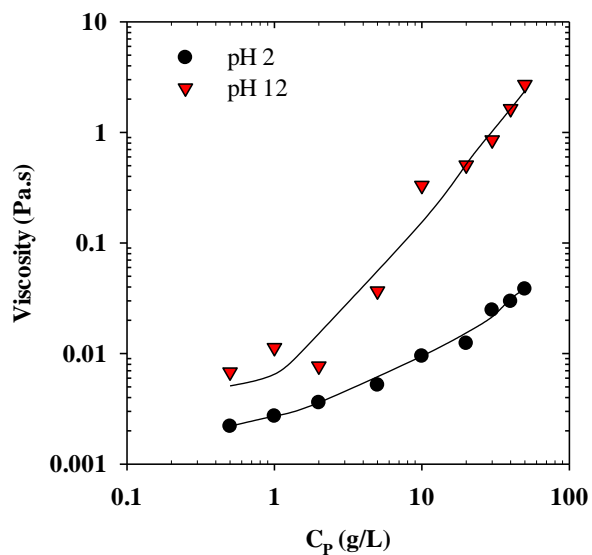
657

658

659

660

661



662

663 **FIGURE 9** Protein concentration dependence of the shear viscosity for FPI solutions at pH 2

664 (circle) and pH 12 (triangle) and at shear rate of 1 s^{-1} . Solid lines are guides to the eye.

665

666

667

668

669

670

671

672

673

674

675

676

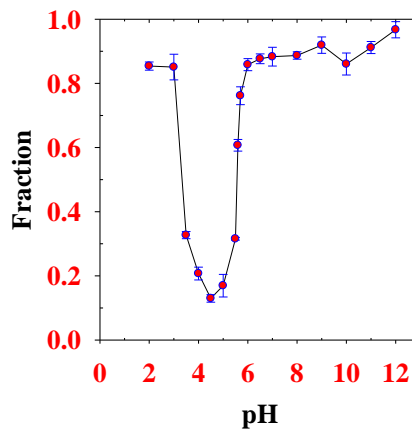
677

678

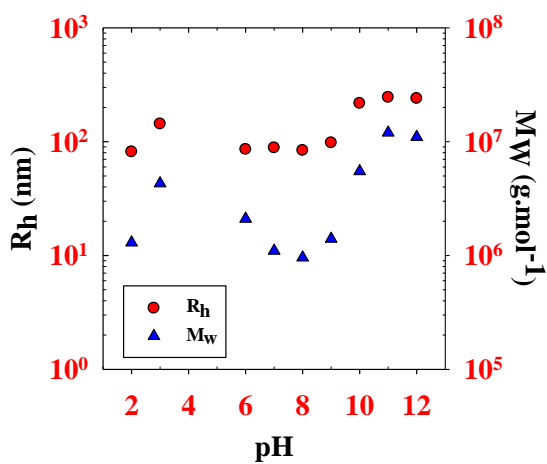
Graphical Abstract



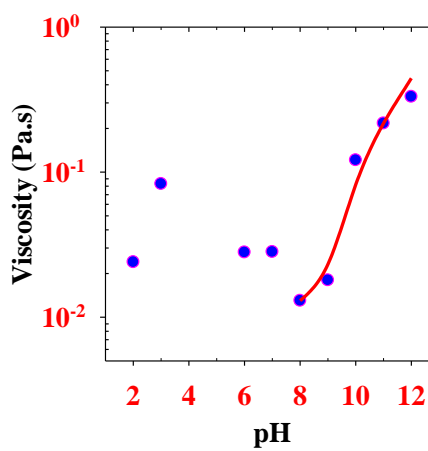
composition



solubility



size



viscosity

679

680

681